# *Ab initio* x-ray absorption study of copper *K*-edge XANES spectra in Cu(II) compounds

Jesús Chaboy
*Instituto de Ciencia de Materiales de Aragón, CSIC-Universidad de Zaragoza, 50009 Zaragoza, Spain*

Adela Muñoz-Páez and Flora Carrera
*Departamento de Química Inorgánica-ICMSE, CSIC-Universidad de Sevilla, 41012 Sevilla, Spain*

Patrick Merkling
*Departamento de Ciencias Ambientales, Universidad Pablo de Olavide, Crta. Utrera Km. 1, 41013 Sevilla, Spain*

Enrique Sánchez Marcos
*Departamento de Química Física, Universidad de Sevilla, 41012 Sevilla, Spain*
(Received 16 November 2004; revised manuscript received 9 February 2005; published 29 April 2005)

This work reports a theoretical study of the x-ray absorption near-edge structure spectra at the Cu *K* edge in several Cu(II) complexes with *N*-coordinating ligands showing a square-planar arrangement around metal cation. It is shown that single-channel multiple-scattering calculations are not able to reproduce the experimental spectra. The comparison between experimental data and *ab initio* computations indicates the need of including the contribution of two electronic configurations ($3d^9$ and $3d^{10}L$) to account for a proper description of the final state during the photoabsorption process. The best agreement between theory and experiment is obtained by considering a relative weight of 68% and 32% for the two absorption channels $3d^{10}L$ and $3d^9$, respectively.

DOI: 10.1103/PhysRevB.71.134208 PACS number(s): 78.70.Dm, 61.10.Ht

## I. INTRODUCTION

X-ray absorption spectroscopy (XAS) has proven to be an outstanding structural tool by allowing the determination of the local environment around a selected atomic species in a great variety of systems.[1] The increasing accuracy of the structural determinations obtained by using XAS is undoubtedly linked to the development of computer simulation codes.[2–11] Most of these codes correspond to theoretical models developed within the multiple-scattering (MS) framework.[12]

At present, reliable structural parameters are commonly derived from the analysis of the extended x-ray absorption fine structure (EXAFS) region of the spectrum. However, the same does not hold for the near-edge part of the absorption spectrum (XANES) despite its higher sensitivity to the bonding geometry. One of the reasons invoked to explain this situation lies in the different influence of the multiple scattering processes in both XANES and EXAFS regions. The low kinetic energy of the photoelectron favors the contribution of multiple scattering processes to the XANES part of the absorption spectrum, so that XANES becomes an incomparable stereochemical probe. However, the absence of an exact treatment of (i) the disorder or vibration effects and (ii) realistic charge densities and their perturbation by the ionization process, among others, makes the *ab initio* computation of the XANES spectra and their analysis no so straightforward as the EXAFS ones.

The search for an accurate description of the XANES region aims new studies focused into the study of the transition metal *K*-edge XANES spectra in simple systems.[13–19] The common goal of these works is to test the improvements of the theoretical computation of XANES, prior to extend the range of applicability of XANES analysis to complex systems. To this respect, while good agreement has been obtained in the case of divalent (Fe, Co, and Ni)[14,15,19] and trivalent (Cr and Rh)[16,17] ions in aqueous solutions, the MS calculations are unable of reproducing the spectral shape in the case of Cu(II).[13] This is a quite disturbing result as copper plays a fundamental role in a great variety of systems, as for example high-$T_C$ superconductors, being also an essential metal cation for many living organisms. Indeed, Cu *K*-edge EXAFS has been widely applied to determine the structure around the metal center in metalloproteins[20] and bioinorganic complexes.[21–23] By contrast, only fingerprint analysis have been conducted in the XANES region. Similar situation is found in the case of high-$T_c$ superconductors and related oxides. While EXAFS leads to the determination of the local lattice distortions in the $CuO_2$ plane of $La_{1.85}Sr_{0.15}CuO_4$,[24] only qualitative information regarding the Cu electronic state has been derived from XANES.[25–27]

In this work, we present a systematic theoretical study of the Cu *K*-edge XANES spectra in several Cu(II) complexes showing a square planar arrangement of increasing complexity around copper. The knowledge of the local environment around absorbing Cu(II) in these complexes, as determined from EXAFS,[28] allow us to test both different choices for the final state potential and the spectrum dependence on the cluster size and on the cluster distortion. In particular, special attention has been paid to establish the improvements obtained by using self-consistent-field (SCF) methods to describe the final state potential and the different treatments of the exchange-correlation part, i.e., $X_\alpha$, Dirac-Hara (DH) and Hedin-Lundqvist (HL) potentials. Our results show the need of including two electronic configurations in the ground state

 

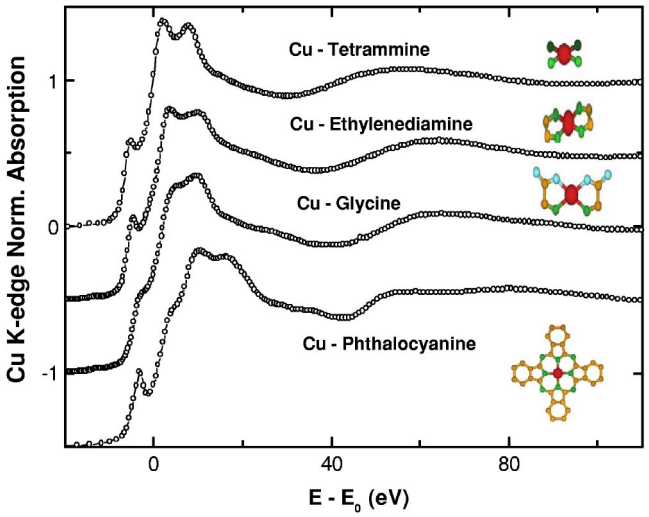


FIG. 1. Experimental XANES spectra at the Cu *K* edge and simplified representation of the structure for the Cu(II) complexes studied (see text for details).

to obtain the agreement between the experimental data and the theoretical calculations.

## II. EXPERIMENTAL AND COMPUTATIONAL METHODS

X-ray absorption experiments were performed at the Cu *K* edge in aqueous solutions of tetramminecopper(II) (hereafter Cu-Tetrammine), bis-ethylenediaminecopper(II) (hereafter Cu-Ethylenediamine), phthalocyaninecopper(II) (hereafter Cu-Phthalocyanine) and bis-glycinatocopper(II) (hereafter Cu-Glycine). XAS measurements were performed at the beamline BM29 of the ESRF. Both XANES and EXAFS spectra were recorded in the transmission mode by using a Si(311) double-crystal monochromator. A detailed description of both sample preparation and the experimental XAS setup can be found in Ref. 28. In all the cases, the origin of the energy scale was chosen at the inflection point of the absorption edge and the spectra were normalized to the averaged absorption coefficient at high energy ($\sim$150 eV above the edge). The experimental XANES spectra, shown in Fig. 1, are in agreement with previously published data.[29–32]

Both FEFF8[9] and CONTINUUM[4] codes were used to calculate the Cu *K*-edge XANES spectra. No significant differences were found for the standard single-channel MS computations obtained by using the two different codes. Hereafter, all the results shown were obtained by using CONTINUUM. In the following we provide a brief outline of the theoretical methods used for the calculations. For a complete discussion of the procedure we refer the reader to Ref. 33.

The computation of the XANES spectra was carried out using the multiple-scattering code CONTINUUM[4] based on the one-electron full-multiple-scattering theory.[5,12] The potential for the different atomic clusters was approximated by a set of spherically averaged muffin-tin (MT) potentials built by following the standard Mattheis' prescription.[35] The muffin-tin radii were determined following the Norman's criterion and by imposing a 10% of overlapping factor.[36] The Coulomb part of each atomic potential was generated using charge densities for neutral atoms obtained from the tabulated atomic wave functions by Clementi and Roetti.[37] The atomic orbitals were chosen to be neutral for the ground state potential, whereas different choices were used to build the final state potential: (i) screened and relaxed $Z+1$ approximation[38] and (ii) self-consistent field potential (SCF). Regarding the exchange and correlation part of the final state potential we have used three different types: $X_\alpha$, the energy dependent Hedin-Lundqvist (HL) complex potential and the energy-dependent Dirac-Hara (DH) exchange potential. The calculated theoretical spectra have been further convoluted with a Lorentzian shape function to account for the core-hole lifetime ($\Gamma=1.5$ eV)[39] and the experimental resolution ($\Gamma=1$ eV).

## III. RESULTS AND DISCUSSION

Systematic *ab-initio* calculation of the Cu *K*-edge XANES spectrum was performed for Cu-Tetrammine, Cu-Ethylenediamine, Cu-Phthalocyanine and Cu-Glycine. This series of compounds corresponds to Cu(II) complexes showing a square planar arrangement around copper of increasing complexity (see Fig. 1). The simplest case is that of four ammine groups, i.e., Cu-Tetrammine, which represents the fourfold coordination of a monodentate ligand. Cu-Ethylenediamine is the example of a tetracoordination built from the twofold coordination of a bidentate ligand. A step beyond is represented by the Cu-Phthalocyanine, a complex where a tetradentated ligand is onefold coordinating the metal cation. Finally, Cu-Glycine represents a twofold coordination, but where the bidentated glycine ligand involves two different coordination atoms, one nitrogen and one oxygen. For each compound, the local environment of Cu used for the XANES computations corresponds to that derived from the EXAFS analysis previously published.[28]

The first calculation was deserved to Cu-Tetrammine as it shows the simplest structure within the series. The local environment around Cu is a square-planar arrangement of four ammine groups, the nitrogen atoms defining a plane which contains the copper cation ($R_{\text{Cu-N}}=2.02$ Å). Figure 2(a) shows the comparison of the experimental XANES spectrum and the calculated ones by using a non-SCF $X_\alpha$ potential for different cluster sizes around the photoabsorbing Cu. The experimental spectrum of Cu-Tetrammine shows several absorption features: (i) a pre-edge peak (A) at ($\Delta E \sim -4.95$ eV); (ii) a split main absorption line (B$\sim$2.3 eV; C$\sim$7.9 eV); (iii) a shoulderlike feature (D) at the high-energy side of the C peak; and finally, (iv) a deep minimum (E$\sim$30 eV) and a broad positive resonance (F$\sim$57 eV) at higher energies. The theoretical calculations reported in Fig. 2(a) do not reproduce the experimental spectrum. Initially, calculation was made by considering only the 4 equatorial *N* next neighbors of Cu. As shown in Fig. 2(a) the main discrepancy between the experimental and the calculated spectrum lies on the shape of the main line resonance. The calculation returns a single line whose width resembles that of

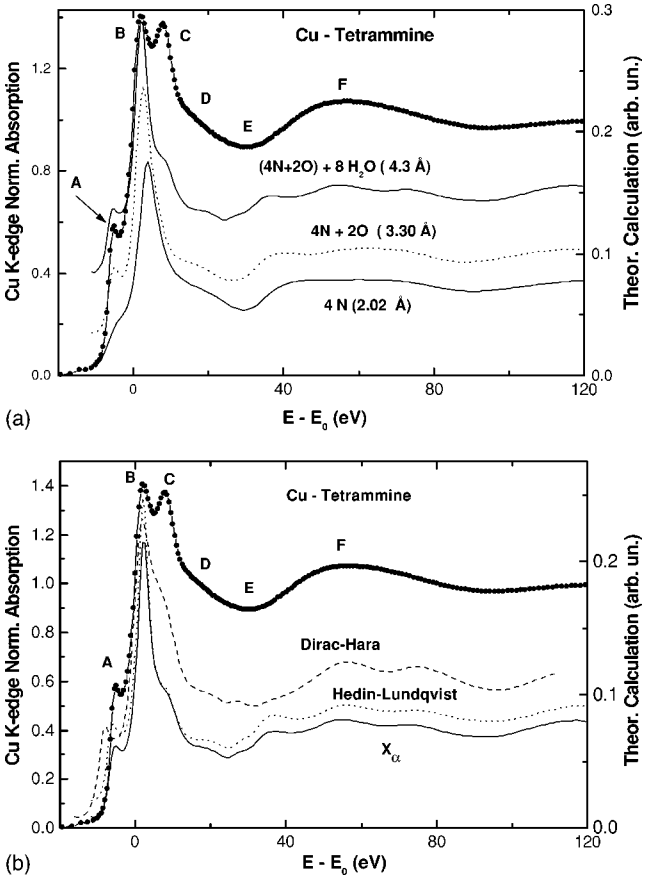


FIG. 2. (a) Comparison of the experimental XANES spectrum at the Cu *K* edge in Cu-Tetrammine (•) and the theoretical spectra calculated by using $X_\alpha$ potential and different cluster sizes (see text for details). (b) The experimental spectrum is compared to computations performed by using different ECP potentials for the greatest built cluster.

peak B. However, no evidence of feature C is reported. No significant improvement of the calculation is obtained by including the two axial oxygen atoms, i.e., the whole distorted octahedron around absorbing Cu. Indeed, while feature A is better reproduced feature C is still missing. The improvement into reproducing feature A is expected because the peak structure at the low energy side of the main line feature is linked to the tetragonal distortion of the octahedron.[40] Finally, we have tested if a second hydration shell formed by eight water molecules tightly bound to the square-planar amino groups can be responsible for the spectral feature C. The result of this calculation is also shown in Fig. 2(a). The inclusion of these oxygen atoms does not account for feature C. The main effect is to produce a shoulderlike structure at the high energy side of peak B, but its intensity is not in agreement with the experimental one. Moreover, while the experimental spectrum exhibits a broad positive resonance (F) at about 60 eV above the edge, the theoretical calculation yields a highly structured feature where at least three peaks can be identified.

The common result of the calculations, performed by using the $X_\alpha$ real exchange and correlation potential, shown in Fig. 2(a), is the failure into reproducing the main line experimental spectral profile, i.e., two peaks with an energy separation $\Delta E \sim 6$ eV. One of the possibilities to improve the theoretical simulation may be the use of different exchange-correlation contributions to the final state potential, due to the fact that they produce modifications on the energy separation between the various resonances. To this aim we have checked the performance of different choices of the exchange-correlation potentials (ECP) into reproducing the experimental spectrum. We have carried out the computation of the Cu *K*-edge XANES spectrum of Cu-Tetrammine by using both the energy-dependent Dirac-Hara (real) and Hedin-Lundqvist (complex) ECP potentials. Moreover, calculations were also performed by (i) convoluting the Dirac-Hara (DH) potential with the imaginary part of the Hedin-Lundqvist (HL) potential (complex DH) and (ii) by taking into account only the real part of the HL potential (real HL). A detailed description of the computational methods can be found in Ref. 33. We report in Fig. 2(b) the comparison between calculations obtained by using different choices of the ECP. Similar unsatisfactory results are obtained by using either $X_\alpha$, or both complex and real HL potentials. None of these ECP is capable of reproducing the splitting of the main absorption line into the two components B and C. The use of the complex DH ECP returns an asymmetric peak at the main line resembling, to some extent, the experimental shape. However, the shoulderlike feature D is missed and both the shape and energy position of the broad resonance F are not reproduced. These results show the failure of these theoretical simulations to account for the XANES spectrum of the $Cu^{2+}$ complex, even with different complex ECP potentials such as Dirac-Hara or Hedin-Lundqvist are used.

The failure of the *ab initio* calculations, specially once we have ruled out all possible structural considerations as the origin of the splitted structure of the main absorption line (peaks B and C), is an unexpected result that compels us to look for an explanation. It has to be stressed that the splitting of the main resonance in peaks B and C is a common feature of several Cu(II) compounds.[23,25,26,29–32,34] Then the following tests have been performed to improve the calculation: (i) more realistic self-consistency field (SCF) potentials and (ii) the incorporation of many-body processes to compute the absorption spectrum.

The $X_\alpha$ self-consistent field (SCF) potential for Cu Tetrammine has been obtained by stabilizing a $[CuN_4]^{10-}$ cluster where the hydrogen atoms are simulated by an outer sphere with a $10^+$ charge to neutralize the whole cluster. Initially, the electronic configuration of Cu(II) has been fixed to the $3d^9$ one. The final state potential was calculated by removing one electron from the 1*s* state and fixing the occupation of this level during the SCF procedure. The result of this calculation is shown in Fig. 3(a). Despite using an improved SCF potential, the obtained computation of the Cu *K* edge of Cu-Tetrammine suffers from the same defects as the non-SCF calculations. Indeed, the double peak structure at the main absorption line is not reproduced and the relative energy between the different experimental spectral features is not well reproduced. Therefore, we have considered the possibility of Cu-Tetrammine XANES spectrum as being due to the superposition of two different excitation channels. Consequently, we have stabilized the SCF potential for two different elec-

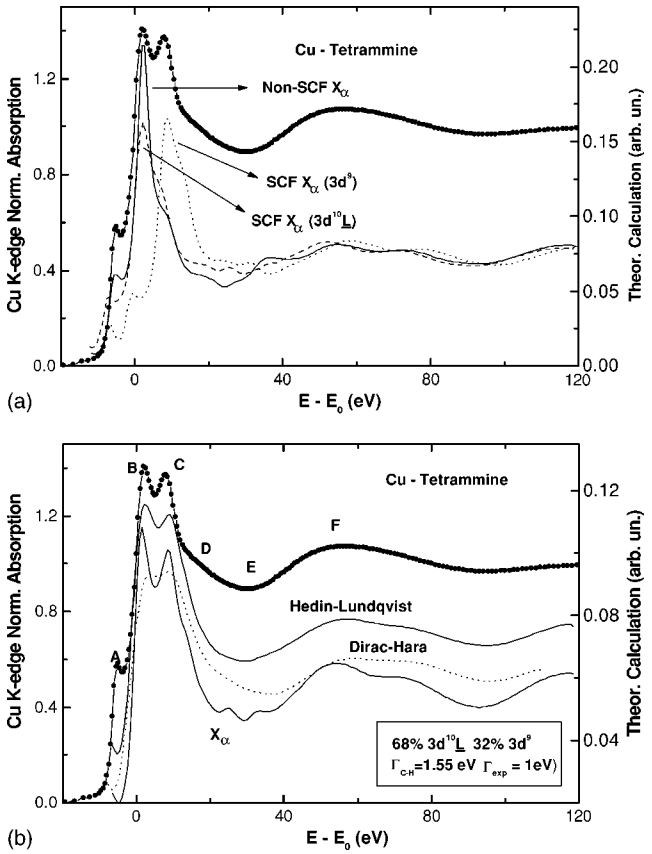


FIG. 3. (a) Comparison of the experimental XANES spectrum at the Cu *K* edge in Cu-Tetrammine (•) and the theoretical spectra calculated by using self-consistent field $X_\alpha$ ECP potentials stabilized for the final-state electronic configurations $3d^9$ and $3d^{10}L$. (b) The experimental spectrum is compared to the theoretical spectra obtained as the weighted sum of the calculation for the configurations $3d^9$ (32%) and $3d^{10}L$ (68%) and by using self-consistent field $X_\alpha$, Hedin-Lundqvist and Dirac-Hara ECP potentials.

tronic configurations $3d^9$ and $3d^{10}L$ ($L$ denoting a hole in $N$ from ligand) in the final state. While in the ground state the $3d^9$ configuration is at lower energy that the $3d^{10}L$ one, the presence of the core hole in the final state shifts the $3d^{10}L$ electronic configuration to lower energy than the $3d^9$. As a consequence, the final state shows a dominant $3d^{10}L$ character. As shown in Fig. 3(a) the two configurations give rise to two absorption edges shifted in energy by $\Delta = 6.37$ eV. This energy difference is very close to the experimental difference, 5.98 eV, between peaks B and C.

The results shown in Fig. 3(a) support the hypothesis of two excitation channels with different excitation energies at the origin of the spectral features observed in Cu-Tetrammine. This procedure is consistent with the sudden limit of the multichannel multiple scattering theory;[41] i.e., the total cross section can be written as a sum of two independent contributions, each of them arising from the two electronic configurations present in the final state. Our findings are in agreement with those obtained by Wu *et al.* in the case of $NdCuO_4$,[42] which confirm the early fingerprint interpretation proposed by Kosugi *et al.*[25,26] The appearance of two competitive ionization channels for Cu(II) has long been reported in x-ray photoelectron spectroscopy (XPS) experiments.[43] Also, shake-down phenomena have been invoked to account for pre-edges structures at the Cu *K* edge of Cu(II) and Cu(III) complexes.[34] Within this framework we have added both contributions with relative weights of 0.68 and 0.32 for the $3d^{10}L$ and $3d^9$ electronic configurations, respectively. As shown in Fig. 3(b), the agreement between both the experimental data and the theoretical simulation is remarkable. In addition, we have also tested the use of different ECP potentials. The main discrepancies of the $X_\alpha$ computation with experiments lie in both the relative intensity of the spectral features and in the calculated absorption maxima falling short of the observed ones. These problems are due, respectively, to the inappropriate treatment of the photoelectron inelastic losses and to the energy independence of the $X_\alpha$ exchange leading to a slight contraction of the calculated spectra. Both problems are solved by using the energy dependent Hedin-Lundqvist ECP, which leads to the best reproduction of the experimental spectrum. By contrast, Dirac-Hara ECP leads to the poorest performance in reproducing the experimental data as the Dirac-Hara self-energy becomes increasingly inadequate at high energies [see Fig. 3(b)]. It should be noted that in order to add the calculations for the two electronic configurations on a unique energy scale it is necessary to shift the energy scale of one spectrum by the difference between the calculated binding energy for the two configurations ($\Delta = 6.37$ eV).[14]

Based on the above results, we have performed the same class of calculations for Cu-Ethylenediamine, Cu-Phthalocyanine and Cu-Glycine. The Cu *K*-edge XANES spectrum of all these compounds is characterized, as in the case of Cu-Tetrammine, by a split main absorption line. Indeed, two peaks are observed at the white line in the case of Cu-Ethylenediamine (Fig. 4), although their intensities are smaller than in the case of Cu-Tetrammine. Similar spectral shape is found for Cu-Phthalocyanine (Fig. 5) which shows in addition a shoulderlike feature ($A_2$) at the low energy side of the white line. Finally, in the case of Cu-Glycine the low energy peak (B) of the main absorption line is depressed as compared to peak C. In all these complexes the local coordination around copper is well established as square-planar,[44] being the first coordination shell formed by 4 nitrogen atoms (2 nitrogen and 2 oxygen atoms in the case of Cu-Glycine), at distances at around 2.00 Å.[28] Despite the presence of a split main absorption line in the experimental Cu *K*-edge XANES spectrum of these compounds is a common result, the relative intensity of the splitted (B and C) peaks is significantly different for the four complexes. Therefore, the *ab initio* calculation of the Cu *K*-edge XANES gives us a good challenge to test the computational procedure used for the Cu-Tetrammine case. Indeed, our main interest is to confirm if the use of two absorption channels to account for the Cu *K*-edge XANES spectrum is a particular request of Cu-Tetrammine or, on the contrary, it is an imperious need for reproducing the Cu *K*-edge spectral shape of all these compounds showing similar square-planar coordination around Cu(II) cations, involving nitrogen-containing ligands.

Figure 4 reports the results of the single-channel calculations performed for Cu-Ethylenediamine. In the case of the non-SCF calculations, the theoretical spectra resemble the

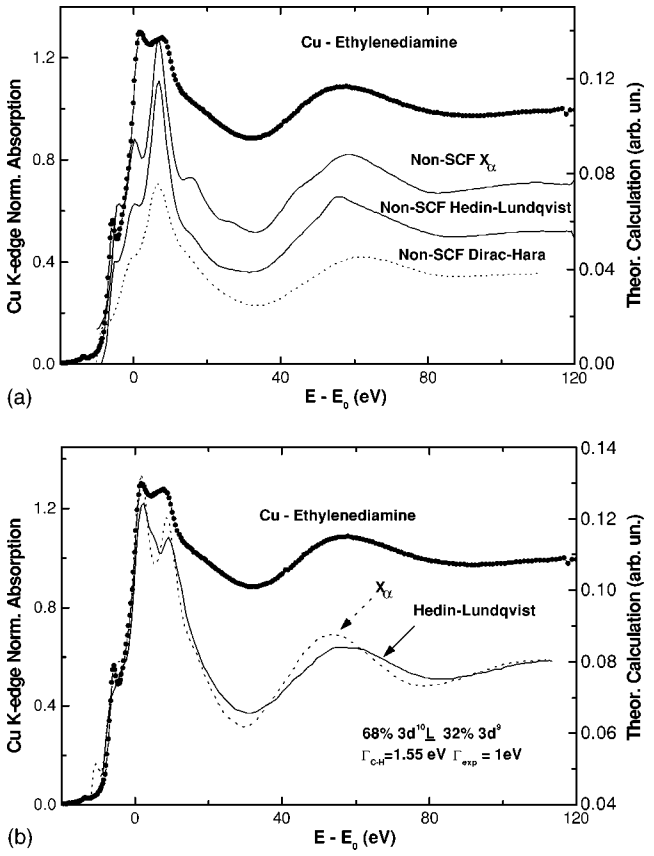


FIG. 4. (a) Comparison of the experimental XANES spectrum at the Cu *K* edge in Cu-Ethylenediamine (•) and the theoretical spectra calculated by using non-SCF $X_\alpha$, Hedin-Lundqvist and Dirac-Hara ECP potentials. (b) Comparison of the experimental spectrum to the theoretical spectrum obtained as the weighted sum of the $3d^9$ (32%) and $3d^{10}L$ (68%) contributions calculated by using the SCF $X_\alpha$ (dotted) and Hedin-Lundqvist (solid line) ECPs.

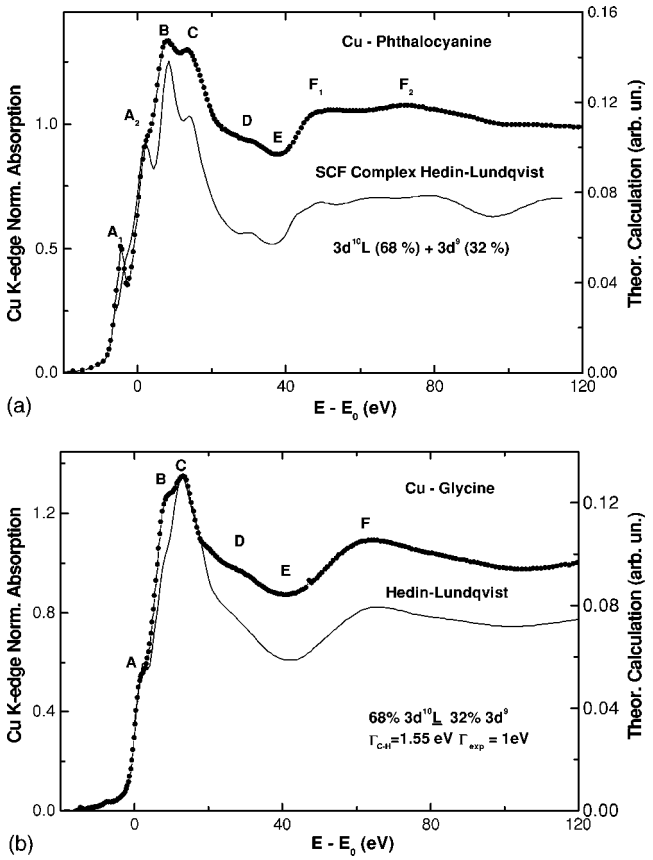


FIG. 5. Comparison of the experimental (•) XANES spectrum at the Cu *K* edge in Cu-Phthalocyanine (a) and Cu-Glycine (b) and the spectra calculated by using two electronic configurations in the final state. The theoretical spectra were built from the weighted sum, 68% and 32%, of the $3d^{10}L$ and $3d^9$ contributions, respectively.

experimental one, with the exception of the main absorption line. The calculation returns a single main line with an additional peak at its low energy side. Despite the energy separation between the various resonances is satisfactory, the relative intensity of the absorption features is not reproduced regardless of the ECP potential ($X_\alpha$, DH or HL) used for the calculation. Therefore, we have applied the same procedure as used for the Cu-Tetrammine computation. We have computed the total cross section as the addition of the contributions associated to the two electronic configurations present in the final state. It should be noted that the relative weight of both configurations has been fixed to 68% for $3d^{10}L$ and 32% for $3d^9$, as in the case of Cu-Tetrammine. With this constraint, the best agreement with the experimental data is shown by the SCF calculation performed by using the complex Hedin-Lundqvist ECP potential [Fig. 4(b)].

The same class of procedure, testing SCF and non-SCF calculations, have been driven for the case of both Cu-Phthalocyanine and Cu-Glycine. As shown in Fig. 5 the use of two absorption channels together with a SCF treatment of the final-state potential and by using a complex HL-ECP leads to a notable agreement between the experimental and the theoretical data. In the case of Cu-Phthalocyanine [Fig. 5(a)] the calculation reproduces the new $A_2$ structure arising at the low energy side of the white line. Moreover, the two structures ($F_1$ and $F_2$) located beyond ~50 eV above the edge are well accounted by the calculation. The good efficiency of the computational procedure is also observed in the case of Cu-Glycine, where the strong modification of the intensity ratio between the two peaks of the main line of the Cu *K*-edge XANES spectrum is well reproduced by the calculation.

Finally, we deserve a special comment regarding the constraint imposed to the relative weight of the two $3d^{10}L$ and $3d^9$ absorption channels. As indicated above, it has been respectively fixed to 68% and 32% through all the comparisons presented here. This was done for the sake of clarity by avoiding the use of any free parameter during the calculations. In this way we have demonstrated the need for including both channels in the four different systems studied. However, it is possible to improve the comparison between experimental and theoretical data by removing this constraint. By taking as a reference the intensity ratio ($R$ =B/C) of the two components of the main absorption line one finds that: in the case of Cu-Ethylenediamine the experimental ratio $R$ is reproduced by using a 60:40 relative weighting for both $3d^{10}L$ and $3d^9$ channels, while it is inverted to 45% and 55% in the case of Cu-Phthalocyanine.

Further work is in progress to get a deeper insight into the relationship between the relative weight of the two electronic configurations present in the final state and the local environment around the absorbing atom. It should be also noted that the presence of two excitation channels has a different impact on both XANES and EXAFS regions. To this respect, it has been verified that an energy difference of at least 15 eV between both channels is needed to get distinguishable contributions to the EXAFS spectrum.

## IV. SUMMARY AND CONCLUSIONS

We have presented the detailed *ab initio* computation of the Cu *K*-edge XANES spectra in the case of several Cu(II) nitrogen-containing complexes (Cu-Tetrammine, Cu-Phthalocyanine, Cu-Ethylenediamine and Cu-Glycine) performed within the multichannel multiple-scattering framework.

The comparison between the experimental Cu *K*-edge XANES spectra of the Cu(II) complexes and the result of the *ab initio* theoretical calculations has shown (i) the one-electron description, in the framework of the muffin-tin multiple scattering theory, is found to be unable to reproduce the Cu(II) experimental data; (ii) the peculiar behavior of the Cu *K*-edge XANES spectra of these complexes can be accounted for by considering a second excitation channel; (iii) the contribution of both $3d^9$ and $3d^{10}L$ electronic configurations have to be taken into account for the correct description of the final state during the photoabsorption process; (iv) best agreement with the experimental data is obtained by using self-consistency field (SCF) potentials and by calculating the total cross section as the sum of two independent contributions, each of them arising from the two electronic configurations present in the final state. It should be stressed that no free parameter has been used during the calculations. In particular, the relative weight of the two absorption channels has been fixed to 68% ($3d^{10}L$) and 32% ($3d^9$) and kept constant during all the computations.

These results, showing the importance of including two different electronic configurations ($3d^{10}L$ and $3d^9$) in the final state, should contribute to a better understanding of Cu(II) *K*-edge XANES. Thus, providing an accurate tool to face the problem of determining the structural environment of Cu(II) cations in complex systems from Cu *K*-edge XANES that is missed to date.

## ACKNOWLEDGMENTS

This work was partially supported by the Spanish CICYT MAT2002-04178-C04-03, BQU2002-02217 and BQU2002-04364-C02-01 grants. ESRF is acknowledged for beamtime allocation at the BM29 line (Experiment number CH-1192). We are indebted to S. Ansell, G. Subías, and S. Díaz-Moreno for their support during the experimental work at ESRF.

[1] For a review see, for example, *X-Ray Absorption: Principles, Applications, Techniques of EXAFS, SEXAFS, XANES*, edited by R. Prins and D. Koningsberger (J. Wiley & Sons, New York, 1988) and references therein.

[2] D. D. Vvedensky, D. K. Saldin, and J. B. Pendry, Comput. Phys. Commun. **40**, 421 (1986).

[3] P. J. Durham, J. B. Pendry, and C. H. Hodges, Comput. Phys. Commun. **25**, 193 (1982).

[4] C. R. Natoli and M. Benfatto (unpublished); M. Benfatto, C. R. Natoli, A. Bianconi, J. García, A. Marcelli, M. Fanfoni, and I. Davoli, Phys. Rev. B **34**, 5774 (1986).

[5] C. R. Natoli and M. Benfatto, J. Phys. (Paris), Colloq. **47**, C8-11 (1986).

[6] T. A. Tyson, K. O. Hodgson, C. R. Natoli, and M. Benfatto, Phys. Rev. B **46**, 5997 (1994).

[7] J. J. Rehr, J. Mustre de Leon, S. I. Zabinsky, and R. C. Albers, J. Am. Chem. Soc. **113**, 5135 (1991); J. Mustre de Leon, J. J. Rehr, S. I. Zabinsky, and R. C. Albers, Phys. Rev. B **44**, 4146 (1991).

[8] S. I. Zabinsky, J. J. Rehr, A. Ankudinov, R. C. Albers, and M. J. Eller, Phys. Rev. B **52**, 2995 (1995).

[9] A. L. Ankudinov, B. Ravel, J. J. Rehr, and S. D. Conradson, Phys. Rev. B **58**, 7565 (1998).

[10] A. Filipponi, A. Di Cicco, T. A. Tyson, and C. R. Natoli, Solid State Commun. **78**, 265 (1991); A. Filipponi, A. Di Cicco, and C. R. Natoli, Phys. Rev. B **52**, 15 122 (1995); A. Filipponi and A. Di Cicco, TASK Q. **4**, 575 (2000).

[11] Y. Joly, Phys. Rev. B **63**, 125120 (2001).

[12] P. A. Lee and J. B. Pendry, Phys. Rev. B **11**, 2795 (1975).

[13] V. Briois, P. Lagarde, C. Brouder, Ph. Sainctavit, and M. Verdaguer, Physica B **208&209**, 51 (1995).

[14] M. Benfatto, J. A. Solera, J García, and J. Chaboy, Chem. Phys. **282**, 441 (2002).

[15] M. Benfatto, J. A. Solera, J. Chaboy, M. G. Proietti, and J García, Phys. Rev. B **56**, 2447 (1997).

[16] P. J. Merkling, A. Muñoz-Páez, and E. Sánchez Marcos, J. Am. Chem. Soc. **124**, 10 911 (2002).

[17] P. J. Merkling, A. Muñoz-Páez, R. R. Pappalardo, and E. Sánchez Marcos, Phys. Rev. B **64**, 092201 (2001).

[18] P. D'Angelo, V. Barone, G. Chillemi, N. Sanna, W. Meyer-Klaucke, and N. V. Pavel, J. Am. Chem. Soc. **124**, 1958 (2002).

[19] P. D'Angelo, M. Benfatto, S. Della Longa, and N. V. Pavel, Phys. Rev. B **66**, 064209 (2002).

[20] R. W. Strange, N. J. Blackburn, P. F. Knowles, and S. S. Hasnain, J. Am. Chem. Soc. **109**, 7157 (1987).

[21] L.-S. Kau, D. Spira-Solomon, J. E. Penner-Hahn, K. O. Hodgson, and E. I. Solomon, J. Am. Chem. Soc. **109**, 6433 (1987).

[22] S. DeBeer, C. N. Kiser, G. A. Mines, J. H. Richards, H. B. Gray, E. I. Solomon, B. Hedman, and K. O. Hodgson, Inorg. Chem. **38**, 433 (1999).

[23] See, for example, R. A. Scott, in *Physical Methods in Bioinorganic Chemistry*, edited by L. Que, Jr. (University Science Books, Sausalito, CA, 2000); I. Ascone, W. Meyer-Klaucke, and L. Murphy, J. Synchrotron Radiat. **10**, 16 (2003) and references therein.

[24] A. Bianconi, N. L. Saini, A. Lanzara, M. Missori, T. Rossetti, H.

Oyanagi, H. Yamaguchi, K. Oka, and T. Ito, Phys. Rev. Lett. **76**, 3412 (1996).
[25] N. Kosugi, Y. Tokura, H. Takagi, and S. Uchida, Phys. Rev. B **41**, 131 (1990).
[26] N. Kosugi, H. Kondoh, H. Tajima, and H. Kuroda, Chem. Phys. **135**, 149 (1989).
[27] See, for example, *High $T_c$ Superconductors, Electronic Structure*, edited by A. Bianconi and A. Marcelli (Pergamon Press, Oxford, 1989).
[28] F. Carrera, E. Sánchez Marcos, P. J. Merkling, J. Chaboy, and A. Muñoz-Páez, Inorg. Chem. **43**, 6674 (2004).
[29] T. I. Morrison, G. K. Shenoy, L. E. Iton, G. D. Stucky, and S. L. Suib, J. Chem. Phys. **76**, 5665 (1982).
[30] S. Bocharov, Th. Kirchner, and C. Dräger, *HASYLAB Annual Report 2000 Part I* (HASYLAB, Hamburg, 2000), p. 299.
[31] P. D'Angelo, E. Botani, M. R. Festa, H.-F. Nolting, and N. V. J. Pavel, J. Phys. Chem. B **102**, 3114 (1998).
[32] G. Lamble, A. Moen, and D. G. Nicholson, J. Chem. Soc., Faraday Trans. **90**, 2211 (1994).
[33] See, for example, J. Chaboy and S. Quartieri, Phys. Rev. B **52**, 6349 (1995), and references therein.
[34] N. Kosugi, T. Yokoyama, K. Asakuna, and H. Kuroda, Chem. Phys. **91**, 249 (1984); T. A. Smith, J. E. Penner-Hahn, M. A. Berding, S. Doniach, and K. O. Hodgson, J. Am. Chem. Soc. **107**, 595 (1985); J. L. DuBois, P. Mukherjee, T. D. P. Stack, B. Hedman, E. I. Solomon, and K. O. Hodgson, J. Am. Chem. Soc. **122**, 5775 (2000).
[35] L. F. Mattheis, Phys. Rev. **133**, A1399 (1964); Phys. Rev. **134**, A970 (1964).
[36] J. G. Norman, Mol. Phys. **81**, 1191 (1974).
[37] E. Clementi and C. Roetti, At. Data Nucl. Data Tables **14**, 177 (1974).
[38] P. A. Lee and G. Beni, Phys. Rev. B **15**, 2862 (1977).
[39] M. O. Krause and J. H. Oliver, J. Phys. Chem. Ref. Data **8**, 329 (1979).
[40] J García, A. Bianconi, M. Benfatto, and C. R. Natoli, J. Phys. (Paris), Colloq. **47**, C8-47 (1986).
[41] C. R. Natoli, M. Benfatto, C. Brouder, M. F. Ruiz López, and D. L. Foulis, Phys. Rev. B **42**, 1944 (1990).
[42] Z. Wu, M. Benfatto, and C. R. Natoli, Phys. Rev. B **54**, 13 409 (1996).
[43] See, for example, *Practical Surface Analysis by Auger and X-ray Photoelectron Spectroscopy*, edited by D. Briggs and M. P. Seah (J. Wiley & Sons, New York, 1983), Chap. 3, pp. 130–131.
[44] A. X. Trautwein, *Bioinorganic Chemistry: Transition Metals in Biology and their Coordination Chemistry* (Wiley-VCH, Weinheim, 1997).